Multiple stages of decay in two-dimensional turbulence

Lei Fang and Nicholas T. Ouellette[a)]

Department of Civil and Environmental Engineering, Stanford University, Stanford, California 94305, USA

We report measurements of the free decay of turbulence in a quasi-two-dimensional laboratory flow. We observe three clearly distinguished stages of decay, each characterized by an exponential decrease of the kinetic energy with time, but with different decay constants. Using filtering techniques, we identify the physics that controls each stage of decay. The first, most rapid stage is not due to the merger of like-sign vortices as has often been suggested but rather to the rapid relaxation of downscale spectral energy leakage. The second stage is a manifestation of dynamical inverse energy cascade processes, and lasts until the separation of scales becomes small. The final stage of decay appears to be dominated by the vertical stratification in our experiment. Our results clarify the dynamical processes at work in decaying two-dimensional turbulence.

[a)]Electronic mail: nto@stanford.edu

I. INTRODUCTION

In many situations in nature, particularly on geophysical scales, flowing bodies of fluid have a very high aspect ratio. In such cases, the dynamics may potentially be considered to be nearly two-dimensional (2D)[1,2]. As is by now well established, two-dimensional turbulence behaves very differently from its three-dimensional counterpart. In 3D, energy moves from the scale at which it is injected into the turbulence toward small scales via the traditional Richardson–Kolmogorov energy cascade[3]. 2D turbulence supports instead the Kraichnan–Leith–Batchelor double cascade[4–6], wherein energy flows to *larger* scales and it is enstrophy that cascades to smaller scales. In this scenario, energy is not removed from the turbulence by viscous effects, but rather only by some large-scale frictional mechanism; and if such a frictional term is not present or not very strong, energy is expected to condense in the largest scales allowed by the geometry[2].

Due to the dynamical transport of energy to large scales in 2D turbulence, there is an expectation that the structure of *unforced* (that is, freely decaying) turbulence in 2D will also be very different from the 3D case. In 3D decaying turbulence, the direct cascade drives the formation of small scale fluctuations that are damped by viscous action; but in 2D, the inverse cascade may potentially create large-scale, long-lived structures that, free of any forcing effects, may persist and interact for long times[1]. Due to this expectation, theories of decaying 2D turbulence have focused on, for example, vortex merger and interaction as the dominant dynamical processes[7–10] or the coupling of large-scale vortex structures to boundaries[11,12]. Much of the previous experimental work, however, was done with relatively coarse resolution by today's standards, and the intervening years have also seen the introduction of new analysis techniques that can be applied to decaying 2D turbulence.

Here, we revisit the problem of decaying 2D turbulence using data from high-resolution laboratory experiments in an electromagnetically driven thin-layer flow. As the flow spins down, we observe three clearly distinguishable stages of decay. Using filter-space techniques that allow us to resolve the scale-to-scale energy fluxes in space and time[13–20], we investigate the physics behind these regimes in detail. We find strong evidence for a decay stage at intermediate times dominated by energy flux through the inverse cascade followed by a final spin-down stage that is dominated by viscous drag and inertia in the overlying fluid layer. The mechanism behind the first, most rapid stage of decay is somewhat less clear, but we

argue that it is likely not due to vortex merger, boundary conditions, or cascade processes but instead appears to be related to the rapid decay of downscale energy leakage. Thus, our results both shed new light on the problem of freely decaying 2D turbulence while also raising some novel, intriguing questions.

We begin below in section II by describing our experimental methods and analysis techniques. In section III, we discuss the results of our work, using both traditional metrics such as the decay of the kinetic energy and more recently developed tools such as spectral energy flux measurements. We also describe the physical mechanisms driving the three stages of decay we observe. Finally, in section IV, we summarize our results.

II. METHODS

A. Experimental details

Our apparatus consists of an electromagnetically driven thin layer of electrolytic fluid with lateral dimensions of 86×86 cm^2. Experiments were performed with a 0.5 cm layer of a solution of 14% by mass NaCl in water, with density $\rho = 1.101$ g/cm^3 and kinematic viscosity $\nu = 1.25 \times 10^{-2}$ cm^2/s. The electrolyte is supported by a smooth flat glass floor coated with a hydrophobic wax to reduce friction. We float an additional layer (about 8 mm deep in these experiments) of fresh water above the electrolyte to create a miscible density interface that sets the plane of the flow we observe.

A square array of 34×34 magnets lies beneath the glass floor. The magnets have diameters of 1.27 cm and thicknesses of 0.32 cm, and are laterally spaced by $L_m = 2.54$ cm. The magnet strength is roughly 600 gauss. The magnets are arranged in stripes of alternating polarity. We pass a controlled DC electric current of 3.22 A laterally through the electrolyte with a pair of copper bar electrodes. The horizontal current and vertical magnetic field produce a Lorentz body force on the fluid, which drives the flow. The current is large enough to produce complex spatiotemporal dynamics and weak turbulence but not so large as to produce significant three-dimensional motion[21]. We define the bulk Reynolds number as $\mathrm{Re} = u' L_m/\nu$ where u' is the in-plane root-mean-square velocity (about 1 cm/s) and $L_m = 2.54$ cm is the magnet spacing. This Reynolds number is essentially a nondimensionalization of the driving electric current[22], and keeping it fixed keeps the statistical properties of the

flow the same from experiment to experiment so that our observations are reproducible. To study decaying flows, we allow the flow to reach a steady state at $\mathrm{Re} = 200$, and then simply turn off the electric current, thereby removing the forcing relatively instantaneously. One can also define an outer-scale Reynolds number $\mathrm{Re}_\alpha = u'/(L_m\alpha)$, where α (with units of inverse time) is a linear damping coefficient that is expected to capture the strength of the dissipation due to the frictional effects of the bottom surface of the apparatus[2]. This Reynolds number should describe the separation of scales in the inverse energy cascade. For steady-state flow in our apparatus at $\mathrm{Re} = 200$, $\mathrm{Re}_\alpha = 8$ (though see section III A for more discussion).

We measure the flow using particle-tracking velocimetry[21,23]. We use 110 μm diameter fluorescent polystyrene tracer particles that are small enough (with a Stokes number of about 2×10^{-4}) to follow the flow accurately[24]. The mass density of the tracer particles lies between those of the electrolyte and the fresh water, and so they remain at the interface. We illuminate the particles with LED lamps and image their motion with a PointGrey Flea3 digital camera operating at 60 frames per second. The camera sensor contains 1280×1024 pixels, and is located 50 cm above the apparatus; the field of view is 24.5×19.3 cm^2 (about $9.5L_m \times 7.5L_m$). We process these images and reconstruct particle tracks using a multiframe predictive particle-tracking algorithm[23]. We record roughly 22,000 particles per frame, so that velocity fields (constructed by projecting the data onto a basis of streamfunction eigenmodes[21]) are well resolved in space.

B. Measurements of spectral energy fluxes

We construct spatial fields of the scale-to-scale energy flux from the raw velocity fields via a filter-space technique (FST)[13–20]. The key to this method is the application of a spectral low-pass filter to the measured fields. This can be done by convolving the measured fields with a kernel $G^{(r)}$ that acts as a low-pass filter in Fourier space with a cutoff length scale of r in real space. The filtered velocity field is given by

$$u_i^{(r)}(x) = \int G^{(r)}(x - x')u_i(x')\mathrm{d}x', \tag{1}$$

where u_i is the i^{th} component of the velocity field and the superscript (r) denotes a quantity with fluctuations at length scales smaller than r suppressed. The equation of motion of the

filtered kinetic energy $E^{(r)} = (1/2)[u_i^{(r)} u_i^{(r)}]$ can be written as[19]

$$\frac{\partial E^{(r)}}{\partial t} = -\frac{\partial J_i^{(r)}}{\partial x_i} - \nu \frac{\partial u_i^{(r)}}{\partial x_j} \frac{\partial u_i^{(r)}}{\partial x_j} - \Pi^{(r)}. \tag{2}$$

The first term on the right hand side of the equation describes the spatial transport of the filtered energy, and the current $J_i^{(r)}$ includes contributions from pressure, advection, and (viscous) diffusion. The second term denotes the direct viscous dissipation of energy at scales larger than r, and is non-positive. Both these terms are analogous to terms in the equation of motion for the unfiltered kinetic energy. The last term is new, and is given by

$$\Pi^{(r)} = -[(u_i u_j)^{(r)} - u_i^{(r)} u_j^{(r)}] \frac{\partial u_i^{(r)}}{\partial x_j}. \tag{3}$$

This final term arises due to the filtering of the nonlinear term. It is a source or sink for the filtered energy, and represents the net energy transfer between the resolved scales (that is, the scales larger than r) and the filtered scales (the scales smaller than r). Given our sign convention, positive values of $\Pi^{(r)}$ indicate energy transfer from larger scales to smaller scales (forward transfer), while negative values indicate transfer from smaller scales to larger scales (inverse transfer). The precise form of the filter kernel $G^{(r)}$ does not have much impact on the results of an FST[16]; in our analysis, we take $G^{(r)}$ to be an isotropic finite impulse response filter constructed from a sharp spectral filter with a cutoff wavenumber of $2\pi/r$ smoothed with a Gaussian window function to reduce ringing.

III. RESULTS AND DISCUSSION

A. Decay of kinetic energy

The simplest way to characterize the decay of the flow is to measure the mean turbulent kinetic energy as a function of time. As the turbulence dies out once the forcing is removed, the kinetic energy must decay with time. In 2D turbulence, the primary energy dissipation mechanism (at least while the turbulence is still relatively well developed) ought to be the large-scale friction rather than the viscosity, as the dynamics preferentially transfer energy to larger scales. In a flow like ours, where this friction primarily arises from the no-slip bottom surface, this effect is usually modeled by the addition of a damping term to the Navier–Stokes equations that is linear in the velocity[2]. This kind of Rayleigh friction would

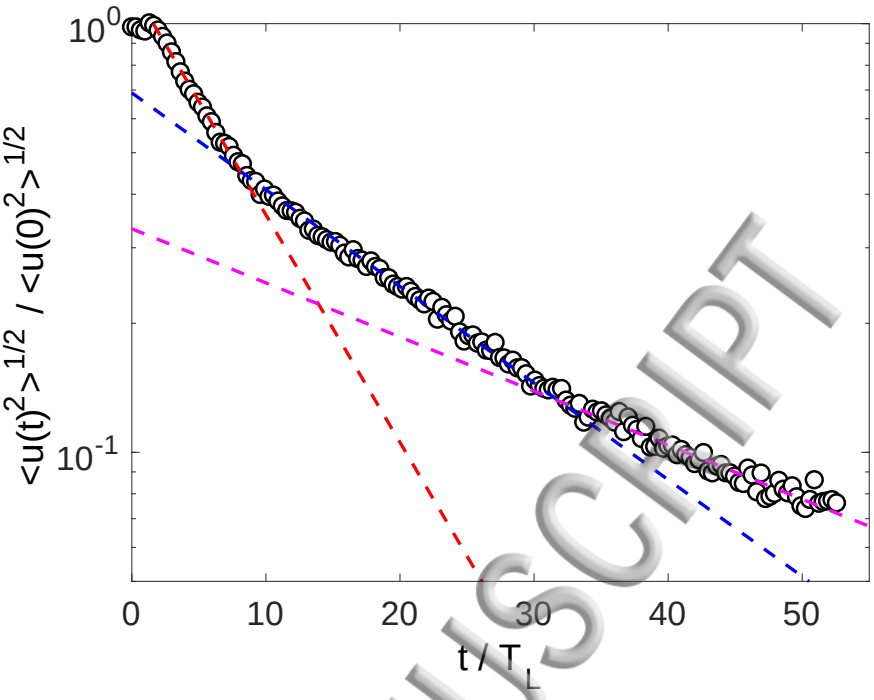

FIG. 1. Decay of the root-mean-square (r.m.s.) velocity in our flow as a function of time, plotted on semi-logarithmic axes. The r.m.s. velocity is normalized by its value at $t = 0$, before the forcing was turned off, and time is normalized by T_L, the characteristic eddy turnover time of the forcing. Three exponential decay regimes are evident. The dashed lines are exponential fits to these regimes, with decay constants of $\alpha^{\mathrm{I}} = (8T_L)^{-1}$ at short times, $\alpha^{\mathrm{II}} = (19T_L)^{-1}$ at intermediate times, and $\alpha^{\mathrm{III}} = (34T_L)^{-1}$ at long times.

then predict an exponential decay of the velocity with time once the frictional damping is no longer globally balanced with an injection of energy; and indeed, in numerical simulations that include such a linear damping, this is precisely what is seen[25].

In fig. 1, we plot the measured root-mean-square (r.m.s.) velocity as a function of time in our flow. We scale the r.m.s. velocity by its steady-state value while the flow was being driven. Shortly after $t = 0$ in fig. 1, we turned off the electric current, and so removed the forcing. Although we do see exponential decay of the r.m.s. velocity, our measurements clearly indicate not one but *three* distinct regimes of exponential decay, with three different decay constants. To distinguish these regimes, we will call them stage I decay, stage II decay, and stage III decay. Fitting the data to curves of the form $\langle u(t)^2\rangle^{1/2}/\langle u(0)^2\rangle^{1/2} \sim \exp(-\alpha t)$, we measure the time constants to be $\alpha^{\mathrm{I}} = (8T_L)^{-1}$ (where $T_L = L_m/\langle u(0)^2\rangle^{1/2}$ is the initial eddy turnover time at the magnet scale) in stage I, $\alpha^{\mathrm{II}} = (19T_L)^{-1}$ in stage II, and

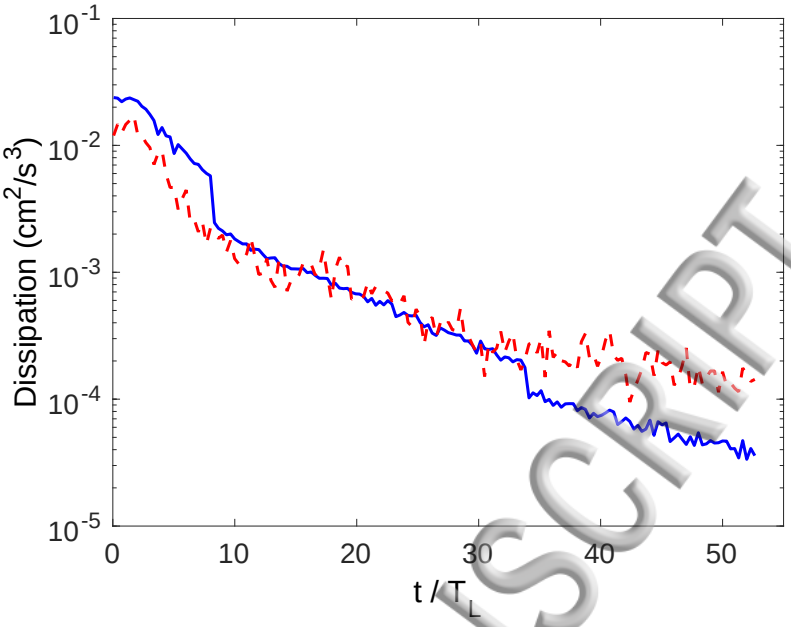

FIG. 2. The energy dissipation rates due to frictional damping (solid line) and viscous effects (dashed line) as a function of time (see text for the definitions of these quantities). In stage I, frictional damping is larger than the viscous effects; in stage II, the two are roughly in balance; and in stage III, viscous effects are stronger than the frictional damping.

$\alpha^{\mathrm{III}} = (34T_L)^{-1}$ in stage III. In determining the outer-scale Reynolds number Re_α defined above, we have used α^{I}, since it quantifies the initial rate of energy dissipation just when the forcing is turned off. Note, however, that we argue below that the decay in stage II is more appropriately associated with the inverse cascade, and so the interpretation of Re_α based on α^{I} as describing the separation of scales in the inverse cascade may be somewhat imprecise. Some previous studies have estimated the bottom friction *a priori* by assuming a Poiseuille profile for the velocity in the vertical direction[10,25–27]; that assumption, however, is inappropriate here since we have no fixed top plate on the apparatus but rather another fluid layer and because our initial flow is turbulent. Finally, we also note that the enstrophy (that is, the square of the vorticity) shows very similar behavior, with three distinct stages of exponential decay with different time constants that are similar, though not identical, to those for the energy.

In a quasi-2D flow like ours, there are expected to be two physical mechanisms for dissipating the kinetic energy: viscous effects and a frictional damping due to coupling to the

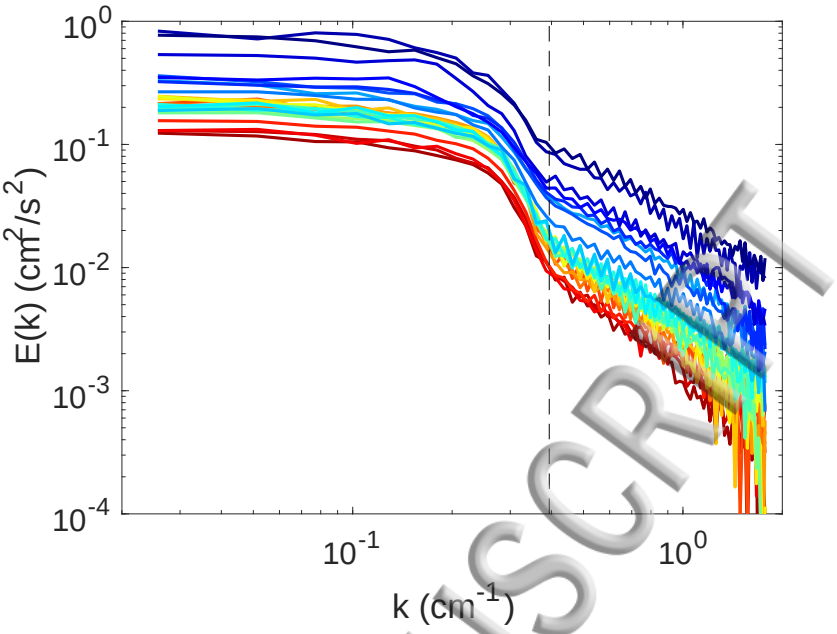

FIG. 3. Energy spectra computed for different times in stages I and II, ranging from $t = 0$ (top) to $t = 33T_L$ (bottom). The vertical dashed line shows the wavenumber associated with the magnet spacing L_m (i.e., $1/L_m$). As the flow decays, the net kinetic energy (given by the integral of the spectrum) decreases.

bottom of the apparatus[2]. The dissipation rate due to viscous damping is, as usual, given by $2\nu s_{ij}s_{ij}$, where s_{ij} is the rate of strain tensor (the symmetric part of the velocity gradient). The dissipation rate due to frictional damping is usually assumed to be given by αu^2, where α is, as above, the decay constant for the kinetic energy—and note that we have three different decay constants, one for each stage of the decay. To try to gain more insight into the physics behind the decay stages we observe, we can compute and compare the viscous and frictional dissipation as a function of time, as shown in fig. 2. We find that in stage I, the frictional damping dominates the viscous dissipation; in stage II, the two are roughly in balance; and in stage III, the viscous dissipation dominates the frictional damping.

In addition to considering only the decay of the kinetic energy and the dissipation, we can also look at how the full energy spectra change in time. We plot the spectra for a range of times in fig. 3. Unsurprisingly, and as we have shown before in this system[20], we do not see a developed inertial range with a $k^{-5/3}$ scaling at any time, given that our Reynolds number is low. For our present purposes, what is relevant to note about the spectra is that the decay

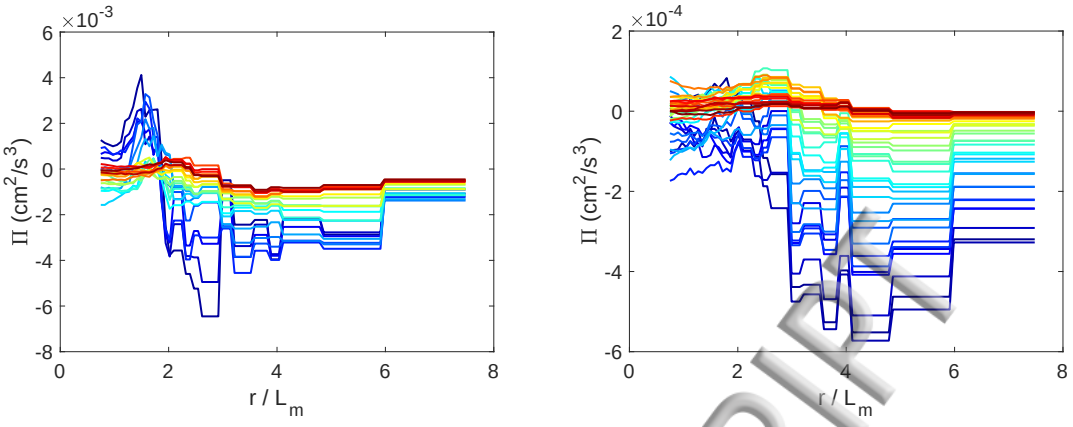

(a) (b)

FIG. 4. Spectral energy flux Π as a function of filter scale r (normalized by the magnet spacing L_m) for different times in stage I (a) and stage II (b). The positive peak at small scales, signifying spectral leakage to small scales, decays rapidly in stage I and is essentially gone by stage II; the flux at other scales decays roughly uniformly with time.

appears to affect all scales more or less equally, as has been seen in other experiments[26]: although the overall kinetic energy decreases (since the integral of the spectrum shrinks), the proportional change in each scale is roughly equivalent with only a small amount of spectral steepening.

Some previous experiments have reported only a single exponential decay[10,26,27] instead the of the three we observe. They were then able to scale out this exponential decay to look purely at how the residual behaved with time, which they then associated with lateral viscous effects. In each of these previous experiments, however, the observation time was significantly shorter than what we have presented; thus, it is possible that our later stages of decay would also have been observable in those experiments as well, had they been run longer. In any case, since we do not observe only a single exponential decay law, there is no reasonable way to compensate our decay results by some assumed form. Thus, to understand in more detail how the decay process works, we require a different analysis tool.

B. Spectral energy fluxes

To gain more insight, we can use the filtering techniques described above to extract the spectral energy flux Π between scales, and see how it varies in time as the turbulence decays.

We plot the spatial mean of these fluxes as a function of filter scale r and for different times (separately plotting times in stages I and II) in fig. 4. Just after the forcing is turned off, the spectral flux has the shape one would expect. Close to the magnet scale L_m, which characterizes (up to an $\mathcal{O}(1)$ constant[28]) the injection of energy into the flow, the spectral flux hits zero. At smaller scales, the mean flux is positive (signifying transfer to smaller scales) near the beginning of stage I, indicating some leakage of energy to small scales[19,29]. As we have shown previously, this leakage is primarily associated with wavevector triads that produce so-called cross stresses[19,20]. For larger scales, the spectral flux is negative (meaning energy transfer to larger scales), consistent with the inverse cascade. Compared to previous measurements we have reported[18–20], there is a here a larger range of scales with a nearly constant flux in this inverse cascade region. We attribute this difference to the removal of pinning effects arising from the spatial layout of the magnets when the forcing is turned off, allowing the flow to evolve more freely and dynamically; additionally, the magnets we used in this experiment were weaker than what we have used in the past[18,21], further reducing their tendency to lock the dynamics of the flow to their pattern[30].

As time progresses, the spectral energy flux decreases at all scales. For scales below the energy injection scale, where we would expect an enstrophy cascade, the positive (leakage) peak in Π decreases noticeably and rapidly in stage I, and is essentially gone by stage II. This rapid decay may be due to the fact that the enstrophy cascade in electromagnetically driven thin-layer flows like ours tends to be relatively weak and incoherent, as opposed to soap-film tunnels, for example[2]. Additionally, some of the cross stresses that are responsible for downscale energy flux[19,20] may be driven by the forcing, and when the forcing is removed these stresses may be able to relax. In the inverse-cascade range, however, the decrease of the energy flux with time is much more uniform; and, similar to what was suggested by the energy spectra (fig. 3), it appears that the energy flux at each scale in the inverse-cascade range decays in roughly the same way.

To make this qualitative observation more concrete, we can choose a single length scale and study how the energy flux at that scale alone changes with time. In general, we find that in the inverse cascade range the flux at a given length scale decays roughly exponentially in time, and that all the scales in the inverse cascade behave in roughly the same way. We can use these findings to try to scale out the changes in the flux as the flow decays, which should allow us to collapse the data. We test this hypothesis in fig. 5. We chose a reference

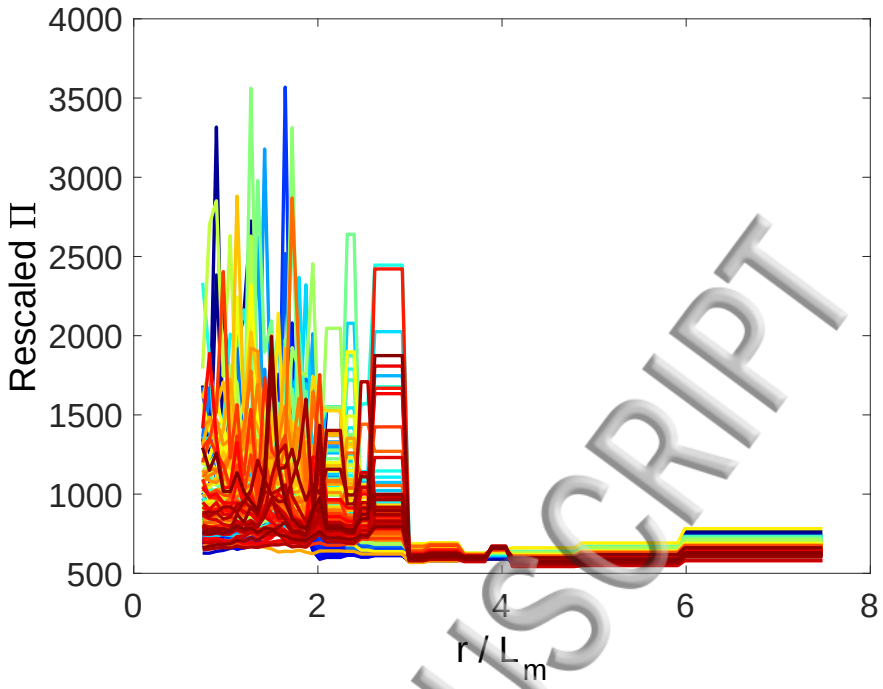

FIG. 5. Spectral flux for $t \in [3T_L, 13T_L]$, rescaled by the exponential decay of the flux at $r = 4L_m$. Data collapse in the inverse-cascade range, indicating that the fluxes at these scales have the same time dependence.

length scale at $4L_m$, and scaled each curve in fig. 4 (all of which are measured at different times) by the instantaneous flux predicted by the exponential decay of the flux at $4L_m$. As one would expect, this re-scaling is poor in the enstrophy range, where the dynamics are relatively incoherent, but works well in the inverse-cascade range.

C. Interpreting the stages of decay

1. Stage I decay

As soon as the forcing is turned off, the kinetic energy begins to decay rapidly over a period of about $8T_L$ (see fig. 1) in what we term stage I decay, before switching over to slower decay. Initial transient decay modes have been observed in previous experiments[8–10] and simulations[12], where they were attributed to the rapid merger of small like-sign vortices into larger vortices. This merger process would lead to the coarsening of the vorticity field, and the generation of larger patches of like-sign vorticity at the expense of the small patches.

To check whether this mechanism is occurring in our flow, we considered the evolution

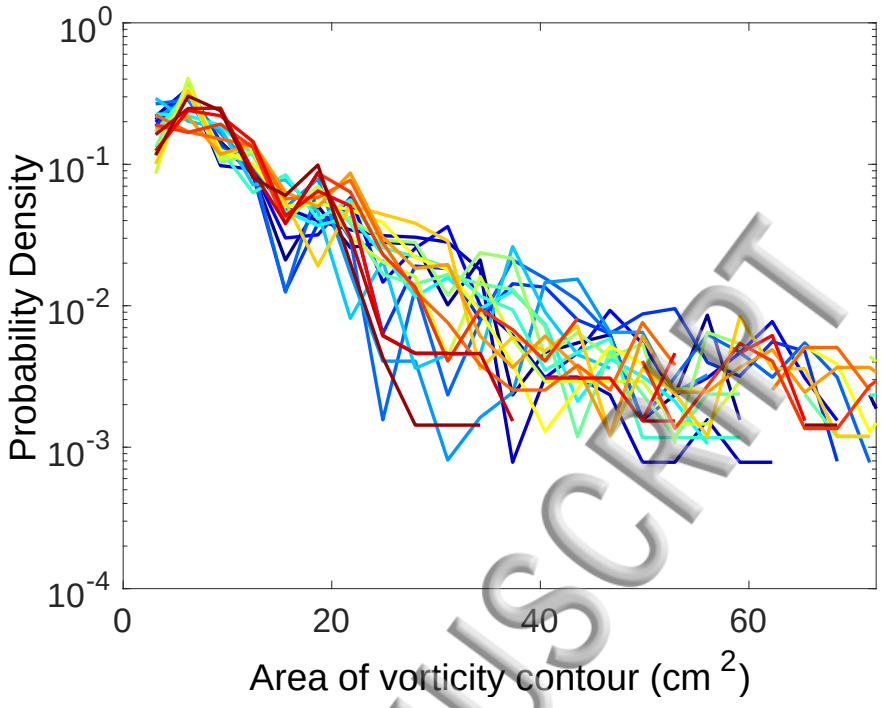

FIG. 6. Probability density functions (PDFs) of the area enclosed by the zero-vorticity contours for a range of times in stage I. No systematic difference or coarsening is seen as time evolves, indicating that like-sign vortex mergers are not playing a significant role in stage I decay.

of the zero-vorticity contours as a way to estimate vortex size[31]. If the vorticity pattern were indeed coarsening due to like-sign vortices merging, one would expect that the areas enclosed by these contours would tend to increase with time. We therefore computed the probability density functions (PDFs) of the area enclosed by the zero-vorticity contours at different times in stage I, as shown in fig. 6. Although these PDFs are noisy (potentially in part because the vorticity contours in 2D turbulence may be highly complex[31]), we observe no trend toward coarsening as the flow decays through stage I, since the PDFs appear to be stationary. We found similar results when using the Okubo–Weiss parameter, which locally compares the magnitude of the vorticity and the strain rate[32,33], to estimate vortex-patch size. Thus, we conclude that stage I decay is not dominated by vortex merger.

In a somewhat different vein, it has also been suggested that the walls of the container can play a nontrivial role in the early stages of decay, potentially leading to a 'spin-up' of the flow due to unbalanced torques at the walls[11,12] that can inject vorticity into the bulk of the flow. This mechanism also does not appear to account for our observations, as we never see any increase in the angular momentum. Additionally, our side walls are very far from

ing measurement area, so that the time it would take for vorticity to diffuse from them into the measurement region is much longer than the duration of stage I decay.

One might expect that stage I may be caused by expected turbulent cascade processes, and that the decay constant α^{I} would simply be related to the frictional damping provided by the no-slip bottom surface. However, as we explain below, there is strong evidence that the inverse cascade is responsible for stage II instead, and there is no reason to expect that the bottom friction should be characterized by two distinct decay constants.

The one process we can identify that appears to occur only in stage I is the leakage of energy from the injection scale to smaller length scales, as is evident from the positive peak in the spectral flux in fig. 4(a) for scales smaller than L_m. This spectral leakage decays rapidly in time, and is essentially gone by the end of stage I, even though the net inverse energy transfer at scales larger than L_m remains. Thus, we conjecture that stage I decay is marked by the rapid relaxation of the downscale spectral leakage of energy (which in turn implies the relaxation of cross stresses driven by the forcing[19,20], which does indeed occur), leading to the establishment of a freely evolving 2D turbulent state.

2. Stage II decay

By the time the decay has reached stage II, after about $8T_L$ (see fig. 1), the initial transient processes have all occurred, and the leakage of energy to scales smaller than the injection scale has significantly reduced (see fig. 4). The flow still retains much of its kinetic energy, however, and the Reynolds number is still high enough that triad interactions are active and the turbulent dynamics can operate. Thus, we interpret stage II as a regime of pure 2D turbulence, with energy transported from small, energy-containing scales to larger scales via the inverse cascade, where it is eventually damped by frictional processes. The signature of the decay in this case is a gradual movement of the effective energy injection scale L_{inj} (marking the "bottom" of the inverse cascade) to larger and larger scales as time goes forward, since energy is transported by the dynamics to larger scales but is not replenished at small scales because there is no forcing. In contrast, the scale of energy dissipation L_{diss} is fixed, as it is set by the apparatus itself and is not dynamical. Thus, as time progresses, the separation of scales between L_{inj} and L_{diss} shrinks until it becomes $\mathcal{O}(1)$, at which point the flow transitions to stage III.

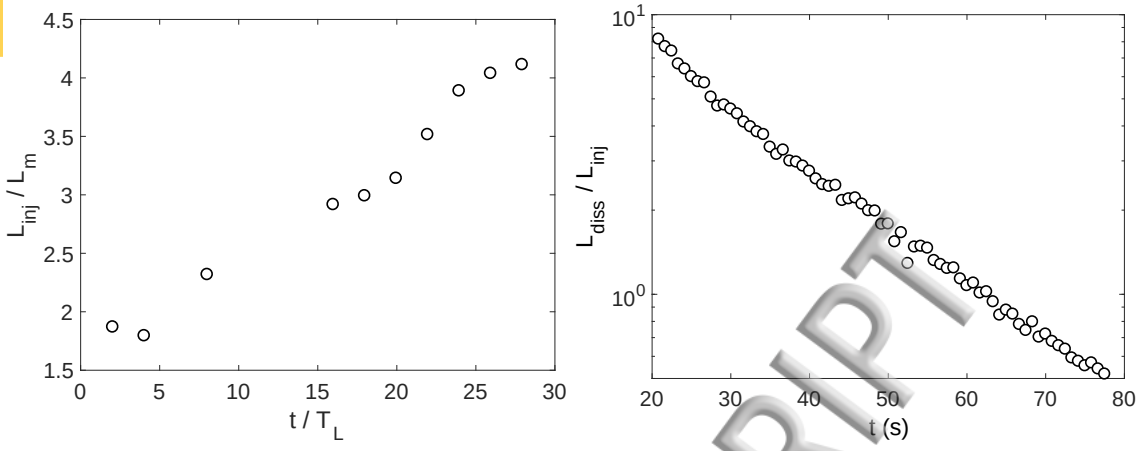

(a) (b)

FIG. 7. (a) Movement of the energy injection scale L_{inj} (see text for definition) with time. (b) Ratio of the dissipation scale L_{diss} (see text for definition) to L_{inj} as time evolves in stage II.

To provide support for this interpretation, we extracted L_{inj} from our spectral flux measurements in fig. 4, defining it as the length scale where Π changes sign as one moves down-scale from the inverse cascade range. In fig. 7(a), we plot L_{inj} (normalized by the magnet scale L_m) as a function of time, and see that it does indeed increase as time progresses. We then estimated the ratio of L_{diss} to L_{inj}, where we defined L_{diss} using the stage II decay constant α^{II} and assuming that the rate of energy injected into the inverse cascade was balanced by the rate of dissipation. As shown in fig. 7(b), this ratio decreases with time until eventually falling below $\mathcal{O}(1)$ near the transition to stage III decay, consistent with our expectations.

3. *Stage III decay*

In the final regime of the decay process, occurring for times longer than about $33T_L$ (see fig. 1), there is almost no kinetic energy left in the flow and the bulk Reynolds number is small. At this point, all turbulent processes have essentially finished, and one no longer expects significant coupling between scales, much as occurs in the final period of decay of wind-tunnel turbulence[34]. In this regime, viscosity can act directly to damp all scales of the motion, and the large-scale friction plays less of a role (see fig. 2). And it has been argued previously from numerical simulation that at very long times, when the flow is nearly a Stokes flow, one should expect an exponential viscous decay of the energy[12].

There is, however, a potential complication for this simple picture in our system: the top fresh water layer. The effects of a top layer have long been a source of debate in the literature. At minimum, its viscosity and density are different from the bottom electrolyte, and so the way its kinetic energy is dissipated may also be different; but since it is also not in contact with the bottom no-slip boundary, it may retain kinetic energy for longer than the electrolyte. Since we measure the flow at the interface between the two layers, it is possible that a more slowly decaying upper layer could potentially act as a source of kinetic energy as sufficiently long times.

To check whether the presence of the top layer impacted the late stage decay of the flow, we conducted additional experiments without the fresh water layer. In this case, we found evidence for the first two stages of decay, but *not the final stage*, suggesting that by the time the turbulent transfer processes had finished, the flow had essentially lost all of its energy. Thus, we conclude that at long times, the remaining inertia in the top layer can indeed feed some energy back into the electrolyte, and this this process is the origin of the late stage decay we see. Thus, this final stage is in some sense an artifact of the particular experimental arrangement rather than a generic effect that will be present in all 2D flows.

IV. SUMMARY

We have here revisited the question of freely decaying two-dimensional turbulence in an experimental system. From measurements of the root-mean-square velocity, we observe three clearly distinguishable decay regimes as the flow spins down. Each of these stages of decay exhibits an exponential decrease of the velocity, but with different decay constants. The first and most rapid stage of decay appears to be associated not with vortex merger processes but rather with the relaxation of the downscale leakage of energy. Once this leakage has disappeared, the flow enters a second stage of decay that is dominated by the expected inverse energy cascade. And finally, once the flow is weak enough that cascade processes are no longer active, the flow enters a final stage of decay that in our flow appears to be heavily influence by the presence of vertical stratification.

ACKNOWLEDGMENTS

This work was supported by the US National Science Foundation under Grant No. CMMI-1563489.

REFERENCES

[1]P. Tabeling, "Two-dimensional turbulence: a physicist approach," Phys. Rep. **362**, 1–62 (2002).

[2]G. Boffetta and R. E. Ecke, "Two-dimensional turbulence," Annu. Rev. Fluid Mech. **44**, 427–451 (2012).

[3]S. B. Pope, *Turbulent Flows* (Cambridge University Press, Cambridge, England, 2000).

[4]R. H. Kraichnan, "Inertial ranges in two-dimensional turbulence," Phys. Fluids **10**, 1417–1423 (1967).

[5]C. E. Leith, "Diffusion approximation for two-dimensional turbulence," Phys. Fluids **11**, 671–673 (1967).

[6]G. K. Batchelor, "Computation of the energy spectrum in homegeneous two-dimensional turbulence," Phys. Fluids **12**, II233–II239 (1969).

[7]G. F. Carnevale, J. C. McWilliams, Y. Pomeau, J. B. Weiss, and W. R. Young, "Evolution of vortex statistics in two-dimensional turbulence," Phys. Rev. Lett. **66**, 2735–2737 (1991).

[8]P. Tabeling, S. Burkhart, O. Cardoso, and H. Willaime, "Experimental study of freely decaying two-dimensional turbulence," Phys. Rev. Lett. **67**, 3772–3775 (1991).

[9]O. Cardoso, D. Marteau, and P. Tabeling, "Quantitative experimental study of the free decay of quasi-two-dimensional turbulence," Phys. Rev. E **49**, 454–461 (1994).

[10]A. E. Hansen, D. Marteau, and P. Tabeling, "Two-dimensional turbulence and dispersion in a freely decaying system," Phys. Rev. E **58**, 7261–7271 (1998).

[11]H. J. H. Clercx, S. R. Maassen, and G. J. F. van Heijst, "Spontaneous spin-up during the decay of 2d turbulence in a square container with rigid boundaries," Phys. Rev. Lett. **80**, 5129–5132 (1998).

[12]H. J. H. Clercx, S. R. Maassen, and G. J. F. van Heijst, "Decaying two-dimensional turbulent in square containers with no-slip or stress-free boundaries," Phys. Fluids **11**, 611–626 (1999).

[13]M. Germano, "Turbulence: the filtering approach," J. Fluid Mech. **238**, 325–336 (1992).

[14]S. Liu, C. Meneveau, and J. Katz, "On the properties of similarity subgrid-scale models as deduced from measurements in a turbulent jet," J. Fluid Mech. **275**, 83–119 (1994).

[15]G. L. Eyink, "Local energy flux and the refined similarity hypothesis," J. Stat. Phys. **78**, 335–351 (1995).

[16]M. K. Rivera, W. B. Daniel, S. Y. Chen, and R. E. Ecke, "Energy and enstrophy transfer in decaying two-dimensional turbulence," Phys. Rev. Lett. **90**, 104502 (2003).

[17]S. Chen, R. E. Ecke, G. L. Eyink, M. Rivera, M. Wan, and Z. Xiao, "Physical mechanism of the two-dimensional inverse energy cascade," Phys. Rev. Lett. **96**, 084502 (2006).

[18]D. H. Kelley and N. T. Ouellette, "Spatiotemporal persistence of spectral fluxes in two-dimensional weak turbulence," Phys. Fluids **23**, 115101 (2011).

[19]Y. Liao and N. T. Ouellette, "Spatial structure of spectral transport in two-dimensional flow," J. Fluid Mech. **725**, 281–298 (2013).

[20]Y. Liao and N. T. Ouellette, "Geometry of scale-to-scale energy and enstrophy transport in two-dimensional flow," Phys. Fluids **26**, 045103 (2014).

[21]D. H. Kelley and N. T. Ouellette, "Onset of three-dimensionality in electromagnetically forced thin-layer flows," Phys. Fluids **23**, 045103 (2011).

[22]D. H. Kelley and N. T. Ouellette, "Using particle tracking to meaure flow instabilities in an undergraduate laboratory experiment," Am. J. Phys. **79**, 267–273 (2011).

[23]N. T. Ouellette, H. Xu, and E. Bodenschatz, "A quantitative study of three-dimensional Lagrangian particle tracking algorithms," Exp. Fluids **40**, 301–313 (2006).

[24]N. T. Ouellette, P. J. J. O'Malley, and J. P. Gollub, "Transport of finite-sized particles in chaotic flow," Phys. Rev. Lett. **101**, 174504 (2008).

[25]B. Jüttner, D. Marteau, P. Tabeling, and A. Thess, "Numerical simulations of experiments on quasi-two-dimensional turbulence," Phys. Rev. E **55**, 5479–5488 (1997).

[26]S. Danilov, F. V. Dolzhanskii, V. A. Dovzhenko, and V. A. Krynov, "Experiments on free decay of quasi-two-dimensional turbulent flows," Phys. Rev. E **65**, 036316 (2002).

[27]H. J. H. Clercx, G. J. F. van Heijst, and M. L. Zoeteweij, "Quasi-two-dimensional turbulence in shallow fluid layers: The role of bottom friction and fluid layer depth," Phys. Rev. E **67**, 066303 (2003).

[28]Y. Liao, D. H. Kelley, and N. T. Ouellette, "Effects of forcing geometry on two-dimensional weak turbulence," Phys. Rev. E **86**, 036306 (2012).

[29]Z. Xiao, M. Wan, S. Chen, and G. L. Eyink, "Physical mechanism the inverse energy cascade of two-dimensional turbulence: a numerical approach," J. Fluid Mech. **619**, 1–44 (2009).

[30]Y. Liao and N. T. Ouellette, "Long-range ordering of turbulent stresses in two-dimensional flow," Phys. Rev. E **91**, 063004 (2015).

[31]D. Bernard, G. Boffetta, A. Celani, and G. Falkovich, "Conformal invariance in two-dimensional turbulence," Nat. Phys. **2**, 124–128 (2006).

[32]A. Okubo, "Horizontal dispersion of floatable particles in the vicinity of velocity singularities such as convergences," Deep-Sea Res. **17**, 445–454 (1970).

[33]J. Weiss, "The dynamics of enstrophy transfer in two-dimensional hydrodynamics," Physica D **48**, 273–294 (1991).

[34]G. K. Batchelor and A. A. Townsend, "Decay of turbulence in the final period," Proc. R. Soc. Lond. A **194**, 527–543 (1948).